SHEAR RESISTANCE MECHANISM OF REINFORCED CONCRETE BEAMS

by Hiroshi Noguchi[I]

SYNOPSIS

In this study sixteen model beams with various pre-formed cracks were designed with the object of analyzing them into their four shear resistant elements: the compression zone of concrete, dowel action of tension reinforcement, aggregate interlock across cracks, and stirrups. The shear force carried by each resistant element was calculated from the detailed strain data to investigate the effect of both a stirrup to arrest the splitting crack and stirrups crossing the inclined crack, on the contributions to the shear capacity of beams of the shear forces carried by the other three resistant elements.

INTRODUCTION

Shear failure has been observed in many short columns of reinforced concrete (RC) buildings subjected to recent severe earthquakes and shear failure has often caused the collapse of RC buildings. The previous studies on shear failure were mostly based on the experimental equations obtained statistically from many test results, or on the crude analytical models only for the strength. But it seems to be very difficult to accunt for shear failure mechanism generally by these means.

The purpose of this study is to investigate the contributions to the shear capacity of RC beams of the shear forces carried by the compression zone of concrete (C), dowel action of tension reinforcement (D), aggregate interlock (A) and stirrups (S), when RC members were subjected to bending moment and shear force due to earthquakes. For this purpose, model beams with various pre-formed cracks were tested with emphasis on the detailed deflection, strain and bond slip measurements.

EXPERIMENTAL PROGRAM

The dimensions of the section are as follows; width, b=20cm; depth, D=30cm; effective depth, d=25cm; tensile reinforcement ratio, p_t=1.55% (2-D22).

The failure mode of Kani's specimens [1] is shown in Fig.1. According to Kani's study [1], the failure mode was not affected so much by the compressive strength of concrete. Therefore Fig.1 is used here as it is. It is considered to be appropriate for the observation on the dowel action and aggregate interlock that the shear span ratio, a/d, is in the range from 1.6 to 2.5 where the strength increases even after the transition from the beam action to the arch action. But when a/d is smaller than 2.0, the crack often occurs along the line between the edges of loading plates. In this case, it becomes difficult to investigate the dowel action. Considering that the actual crack pattern is affected by the width of the loading plate, 2.0 ~ 2.4 is selected as the range from a_e/d to a/d in order

I Associate Professor, Faculty of Engineering, Chiba University, Chiba, Japan

to fulfill the requirements above mentioned. (a_e: the distance between the edges of loading plates)

Bower et al. represented the distance a_c, shown in Fig.2, between the intersection of the initial inclined crack with the tension reinforcement and the section of zero moment by the following experimental equation. [2]

$$a_c/d = 0.241 + 0.117a/d + 0.0756\ (a/d)^2 \qquad (1)$$

a_c was set as 24cm for this test series from Eq. (1).

The inclined crack is idealized by the tri-linear curve shown in Fig.2. The variables which prescribe the inclined crack pattern were decided by curve fitting it to the previous test data by Kani [1] and other researchers, as follows. $\theta_2 = 43°$, $x_L/D = 0.198$, $\theta_3 = 21.4°$, $x_N/D = 0.148$. θ_3 and x_N/D were given by the following equations.

$$\theta_3 = -6.4a/d + 36.8 \qquad (2)$$

$$x_N/D = -0.07a/d + 0.31 \qquad (3)$$

Calculated inclined crack patterns for Kani's specimens, are shown in Fig.3 by dashed lines. Calculated crack patterns indicate substantial agreement with experimental crack patterns for $a/d = 2 \sim 3$, including other specimens.

Sixteen model beams, shown in Fig.4, were composed of the following four series.

Series 1: 4 beams. This series was carried out to investigate the shear resistance mechanism of beams without a stirrup. No.1 was a non-formed crack specimen. For No.2, the slit was made to induce the inclined crack and the flexural one. Therefore No.2 was carried by (C), (D) and (A). For No.3, the inclined crack and the flexural one were pre-formed and the crack width was set as 0.1mm. No.3 was carried by (C) + (D). For No.4, the roller was put in at the compression zone of the same specimen as No.3. No.4 was carried only by (D).

Series 2: 4 beams. This series was carried out to study the effect of a stirrup placed at 5cm distance, f = 5cm, from the incined crack on the support side. In other respects, this series was corresponding to series 1. The lower part of each specimen's number was corresponding to series 1. (So with series 3,4)

Series 3: 4 beams. This series was carried out to investigate the shear resistance mechanism of beams with both stirrups crossing the inclined crack and the same stirrup as series 2, except No.63. The stirrup ratio, p_w, of No.22, No.23 and No.63 was corresponding to the Arakawa's minimum equation. ($p_w = 0.64\%$) [3] p_w of No.33 was corresponding to the Arakawa's original equation. ($p_w = 0.43\%$)

Series 4: 4 beams. This series was carried out to study the effect of the combination of a stirrup crossing the inclined crack and a stirrup, f = 10cm, in the case of shear failure.

The crack was pre-formed on the one side of the specimen and the other side was reinforced in order not to fail in shear.

The compressive strength of concrete, f'_c, was 163 ~ 262 kg/cm^2 and the yielding strength of the reinforcement was 3786 ~ 3906 kg/cm^2 for the tension reinforcement, D22, and 3286 ~ 3515 kg/cm^2 for the stirrup, 9ϕ.

The beams were loaded with two concentrated loads. The measurements taken on each beam were: deflections, strains of reinforcing bars and concrete, bond slip measured by the direct method, and observation of cracks.

PROGRESS OF FAILURE

Load-deflection relationships for each series are shown in Figs.5 ~ 8. Inclined crack patterns for No.1 and No.11 indicate substantial agreement with calculated crack patterns except the location of crack initiation for No.11.

Series 1. Three specimens, No.1, 2, 3, failed in shear compression after the splitting crack along the tension reinforcement. No.4 attained the maximum strength when the splitting crack occurred.

Series 2. Three specimens, No.11, 12, 13, failed in shear compression. The stiffness deterioration of No.11 without a stirrup after the splitting crack was remarkable. The effect of aggregate interlock on load-deflection curves did not come out from the comparison of No.12 with No.13. Comparing the dowel specimen No.14 with No.4 in series 1, it was confirmed that the presence of a stirrup near to the crack (f=5cm) enlarged the dowel stiffness after the splitting crack and the dowel strength was nearly equal to the strength of a stirrrup.

Series 3. All specimens failed in flexural compression without the yielding of stirrups. The aggregate interlock had almost no effect on the load-deflection curves from the comparison of No.22 with No.23.

Series 4. Three specimens, No.53, 42, 43, failed in shear compression with the yielding of stirrups crossing the inclined crack. In No.53, the test data from P = 4t to 10t under virgin loading was not available for the loading trouble. The dowel strength of No.44 was nearly equal to the strength of the tension reinforcement in beam action without the yielding of a stirrup.

CONTRIBUTIONS OF SHEAR RESISTANT ELEMENTS

In the reinforced concrete beam after the inclined crack occurred, the total shear force was carried by the compression zone of concrete (C), dowel action of the tension reinforcement (D), aggregate interlock (A), and stirrups crossing the inclined crack (S).

The shear force, Qs, carried by (D) was calculated from the rosette strain of the tension reinforcement at the intersection of the inclined crack with the tension reinforcement, as shown in Fig.9.

The shear force, Qc, carried by (C) was calculated as follows. The shear stress, τ_{xy}, was obtained by the nonlinear rosette analysis based on the Darwin's constitutive law under biaxial stresses [4], from the

rosette strain at the median point in the compression zone, as shown in Fig.9. The shear stress distribution in the compression zone was assumed to be constant on the ground that the measured rosette strain was average.

Figs.10 - 24 show plots of the total shear force Q, Qs and Qc, against the deflection at the loading point.

Series 1. In No.2, after the inclined crack has been propagated along the pre-formed slit, Qc increases gradually from Qc/Q=53% to 85%, as shown in Fig.10. Qs increases gradually and after the splitting crack occurs, Qs/Q is about 20%. Regarding {Q-(Qc+Qs)} as Qa, the shear force carried by (A), Qa decreases gradually from Qa/Q=30% to 0% with the opening of the inclined crack. In No.3 Qa is about zero for the smoothness of the pre-formed crack surface, as shown in Fig.11. In the dowel specimen No.4, Qs/Q is about 100% and Qc/Q is about 0%, as shown in Fig.12. From the comparison of No.4 with No.2, 3 about the strength, Qs/Q is 16 ~ 20% and it corresponds to the ratio, 20% obtained from the rosette analysis.

Series 2. In No.11 without stirrups, Q and Qc are corresponding to those in No.2, as shown in Figs.13 and 10. In No.12 Qc/Q is 60 ~ 76% after the inclined crack has been propagated, as shown in Fig.14. Qs/Q is 13 ~ 17% after the splitting crack occurs. Qa/Q decreases from the maximum ratio Qa/Q=27% to about 0% nearly at the maximum strength. In No.13, Qc/Q is 30 ~ 42% and Qs/Q is 62 ~ 69%, as shown in Fig.15. In the dowel specimen No.14, Qc/Q is fairly small, but Qs does not obtain a good result for the difficulty in the case of the large dowel deflection, as shown in Fig.16. The maximum strength of No.14 is decided by both the yielding of a stirrup and the strength of the tension reinforcement in beam action. The shear force, Q_h, carried by a stirrup is plotted in Figs.14 ~ 16. For No.13, 14, Q_h is nearly equal to Qs after the splitting crack occurs, as shown in Figs. 15, 16. If Qs is equal to Q_h also for No.12, Qs/Q comes to be 10 ~ 53% and Qa/Q is less than 10%, as shown in Fig.14. This is corresponding to the fact that the effect of (A) on the load-deflection curve does not come out.

Series 3. The shear force, Q_h, carried by stirrups crossing the inclined crack and Q_{h0}, carried by a stirrup near to the inclined crack, are plotted in Figs.17 ~ 24. In No.22, the ratios Q/Q_{total} are as follows, (C):30%, (D):18%, (A):16%, (S):36% at Q=7.3t when the inclined crack has been propagated along the slit, as shown in Fig.17. Nearly at the maximum strength, Q_{max} in No.22, 23 (stirrup ratio p_w=0.64%), Q/Q_{total} are as follows, (C):38 ~ 57%, (D):13 ~ 16%, (A):0%, (S):53 ~ 58%, as shown in Figs. 17, 18. In No.33 (p_w=0.43%), nearly at Q_{max}, Q/Q_{total} are as follows, (C):58%, (D):4 ~ 6%, (A):0%, (S):42%, as shown in Fig.19. The effect of the decrease in p_w appears in the increase in (C) and the decrease in (S). In No.43 (p_w=0.64%), the location of stirrups is different from No.22, 23, as shown in Fig.4. Nearly at Q_{max}, Q/Q_{total} are as follows, (C):40%, (D): 0%, (A):0%, (S):58%, as shown in Fig.20.

Series 4. In No.53 with a stirrup crossing the inclined crack, nearly at Q_{max}, Q/Q_{total} are as follows, (C):58%, (D):12%, (A):0%, (S):37%, as Shown in Fig.21. In No.42, Q/Q_{total} are as follows, (C):16%, (D):20%, (A): 44%, (S):19% at Q=5.8t when the inclined crack has been propagated along the slit, as shown in Fig.22. Nearly at Q_{max}, Q/Q_{total} are as follows, (C):53%,

(D):20%, (A):0%, (S):34%. In No.43, nearly at Q_{max}, Q/Q_{total} are as follows, (C):46%, (D):17%, (A):0%, (S):36%, as shown in Fig.23. In the dowel specimen No.44, Oc/Q is fairly small, as shown in Fig.24. Qs is considerably conservative under the lower load, but comes up to Q nearly at Q_{max}. Q_{max}=3.2t is nearer to the strength of the tension reinforcement in beam action, Q=2.60t, than the yielding strength of a stirrup, Q=4.18t.

CONCLUSION

Sixteen model beams were tested to study the effect of stirrups on the contribution to the shear capcity of RC simple beams of each resistant element: the compression zone of concrete, dowel action of tension reinforcement and aggregate interlock.

These test data are available for the subject of finite element analysis and it will be necessary to investigate the shear resistance mechanism of RC members not only by the experimental studies but also by the analytical studies.

ACKNOWLEDGEMENTS

This study was supported by the Japan Building Center and the Tokyo Electric Power Company. The author wishes to express his deepest gratitude to Professor Emiritus H. Umemura and Professor H. Aoyama at the University of Tokyo for their warmhearted guidance.

REFERENCES

1) Kani, G.N.J.,"The Riddle of Shear Failure and Its Solution," ACI Journal, Vol. 61, April 1964, pp.441 - 467.

2) Bower, J.E. and Viest, I.M.,"Shear Strength of Restrained Concrete Beams without Web Reinforcement," ACI Journal, Vol.57, July 1960, pp.73 - 98.

3) Arakawa, T.,"Allowable Unit Shearing Stress and Design Method of Shear Reinforcement of Reinforced Concrete Beams, Analyses of Existing Test Data," Concrete Journal, Vol. 8, No.7, July 1970, pp.11 - 20.

4) Darwin, D. and Pecknold, D.A.W.,"Inelastic Model for Cyclic Biaxial Loading of Reinforced Concrete," SRS No.409, Civil Engineering Studies, Univ. of Illinois, July 1974, pp.1 - 169.

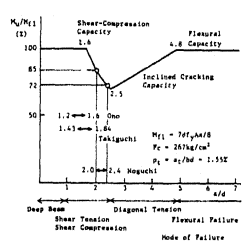

Fig.1 Failure Mode of Kani's Specimens

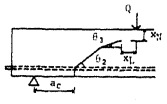

Fig.2 Location of Inclined Crack

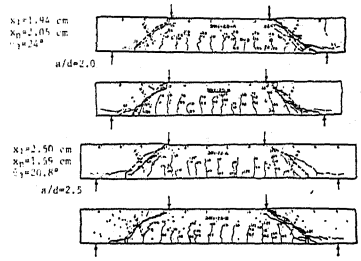

Fig.3 Crack Patterns in Beams Tested by Kani

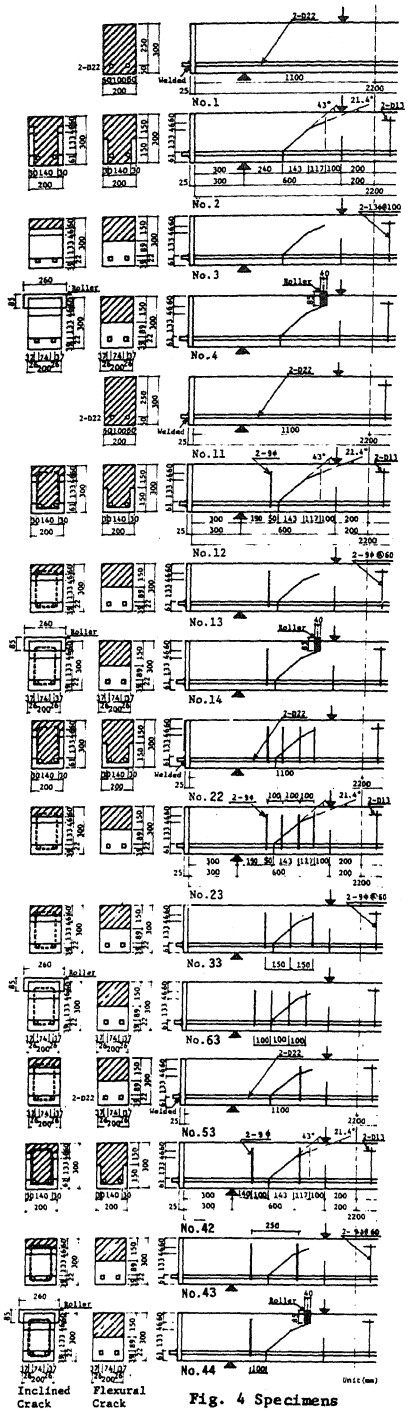

Fig. 4 Specimens

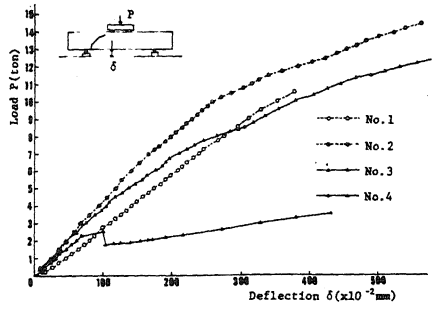

Fig. 5 Load-Deflection Relationships (Series 1)

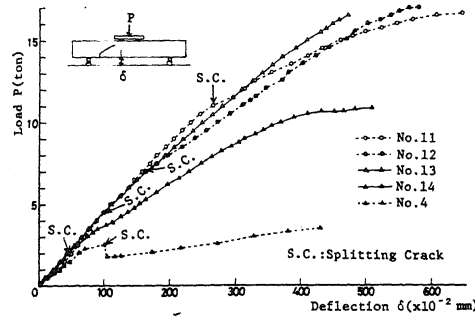

Fig. 6 Load-Deflection Relationships (Series 2)

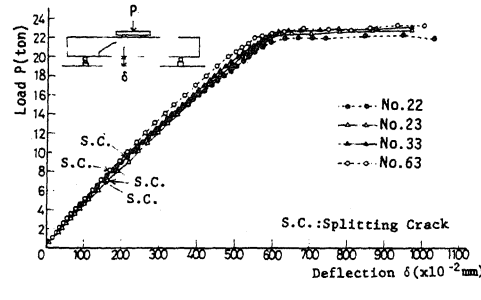

Fig. 7 Load-Deflection Relationships (Series 3)

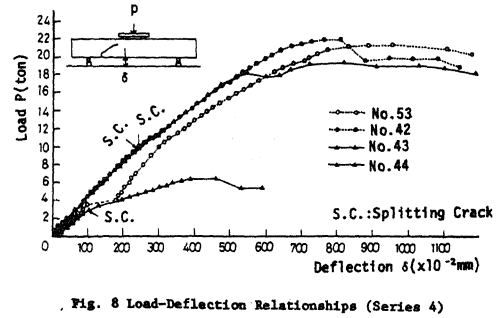

Fig. 8 Load-Deflection Relationships (Series 4)

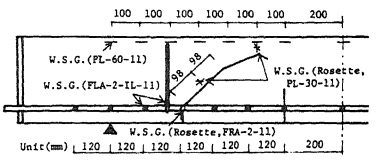

Fig. 9 Positions of Wire Strain Gauges on Tension Reinforcement, Stirrup and Concrete

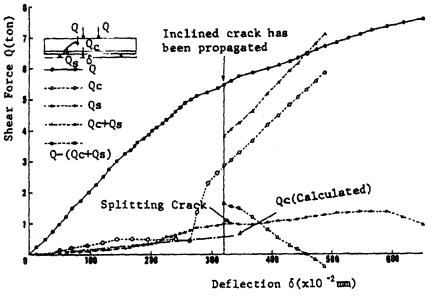

Fig. 10 Shear Force-Deflection Relationships (No.2)

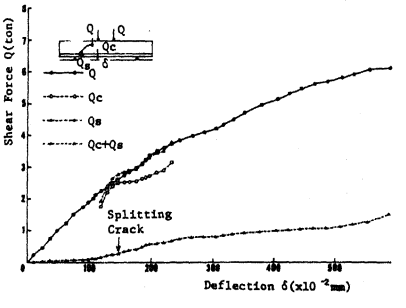

Fig. 11 Shear Force-Deflection Relationships (No.3)

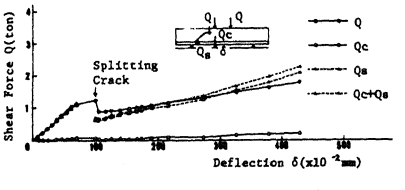

Fig. 12 Shear Force-Deflection Relationships (No.4)

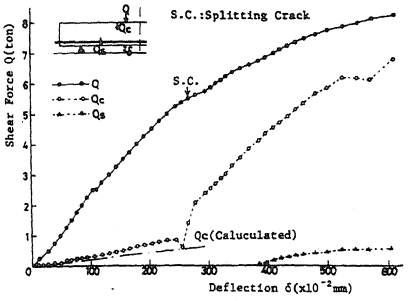

Fig. 13 Shear Force-Deflection Relationships (No.11)

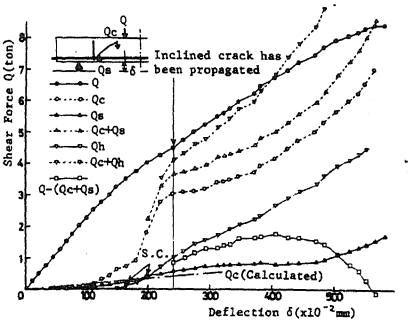

Fig. 14 Shear Force-Deflection Relationships (No.12)

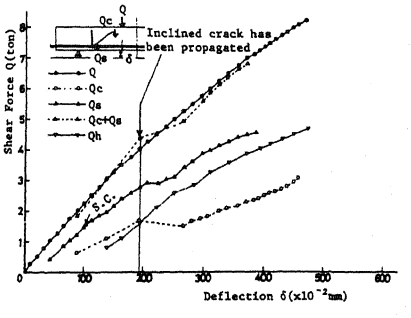

Fig. 15 Shear Force-Deflection Relationships (No.13)

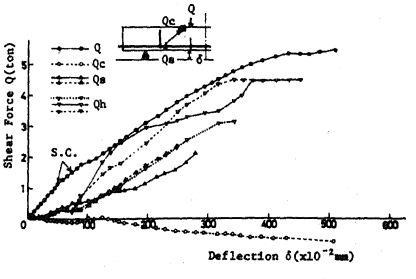

Fig. 16 Shear Force-Deflection Relationships (No.14)

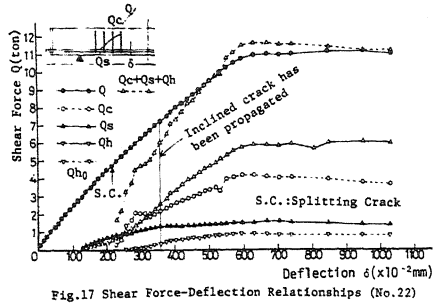

Fig.17 Shear Force-Deflection Relationships (No.22)

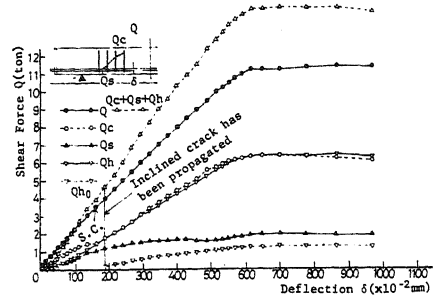

Fig.18 Shear Force-Deflection Relationships (No.23)

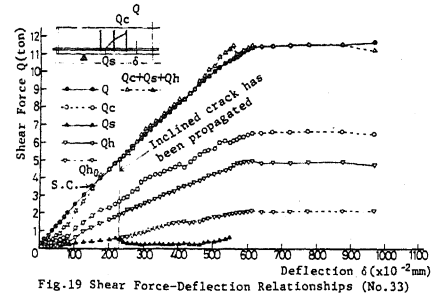

Fig.19 Shear Force-Deflection Relationships (No.33)

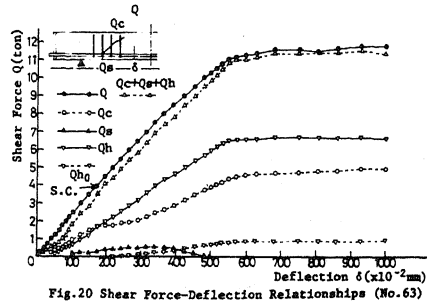

Fig.20 Shear Force-Deflection Relationships (No.63)

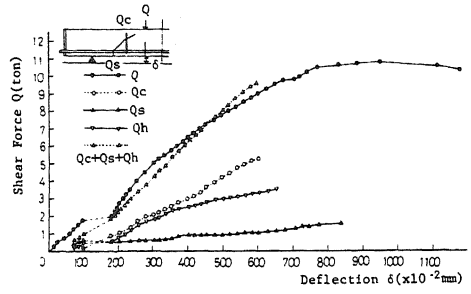

Fig.21 Shear Force-Deflection Relationships (No.53)

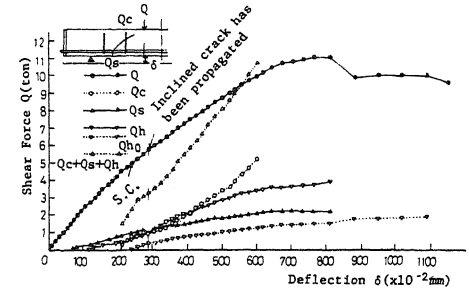

Fig. 22 Shear Force-Deflection Relationships (No.42)

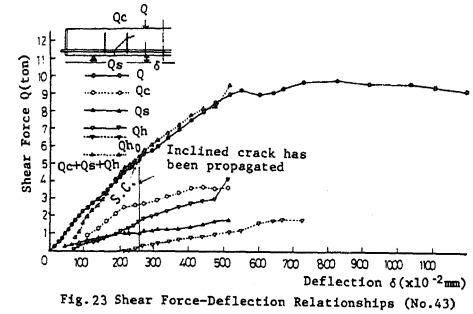

Fig. 23 Shear Force-Deflection Relationships (No.43)

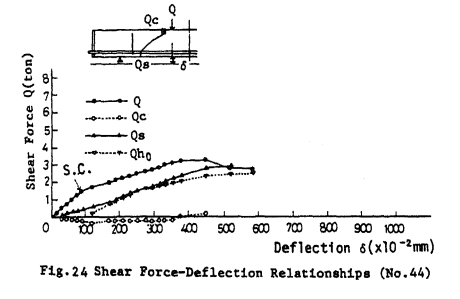

Fig.24 Shear Force-Deflection Relationships (No.44)